Biochemical and clinical effects of RPS20 expression in renal clear cell carcinoma

CHENG SHEN[1,2*], ZHAN CHEN[1,2*], YONG ZHANG[1,2], WEI XU[1,2], RUI PENG[1,2],
JIE JIANG[1,2], WENJING ZUO[3], YIHUI FAN[4] and BING ZHENG[1]

[1]Department of Urology, [2]Medical Research Center and [3]Department of Orthopedics,
The Second Affiliated Hospital of Nantong University; [4]Department of Pathogenic Biology,
School of Medicine, Nantong University, Nantong, Jiangsu 226001, P.R. China

Abstract. Renal cell carcinoma (RCC) remains one of the most lethal urinary tumors in East Asia despite great advancements in treatment strategies in recent years. Ribosomal protein S20 (RPS20) is considered a new oncogene; however, little information is available on its expression, regulation and biological function in patients with RCC. In the present study, 43 pairs of human RCC and neighboring normal renal tissues were examined for protein expression and immunohistochemistry examination of RPS20. Lentiviral transduction was also employed to create RPS20 knockdown cell lines for downstream cellular experiments. MTT, flow cytometry, wound healing, colony formation and invasion assays were used to examine how RPS20 affected kidney renal clear cell carcinoma (KIRC) cell behavior. Western blotting was used to detect cycle-related proteins (CDK4 and cyclin D1), Wnt-related proteins (N-cadherin and E-cadherin) and signaling proteins [phosphorylated (p)-AKT and p-ERK]. The functions of RPS20 *in vivo* were examined in 786-O cells with RPS20 knockdown. RPS20 was significantly overexpressed in tumor tissues compared with its expression in the corresponding normal tissues. RPS20 expression was linked to tumor stage, differentiation grade, tumor size and lymph node metastasis, and it had an independent prognostic value in KIRC. Since RCC cell proliferation, migration and invasion were suppressed when RPS20 was knocked down, the formation of renal tumors *in vivo* was markedly slowed down. In RPS20 knockdown cell lines, CDK4, cyclin D1 and E-cadherin were downregulated, while N-cadherin expression was increased. RPS20 was also observed to be involved in controlling the activation of the ERK and mTOR signaling pathways. In summary, the present study showed that RPS20 increased cell proliferation in RCC by activating the AKT-mTOR and ERK-MAPK signaling pathways, which suggests that RPS20 may be a therapeutic and prognostic target for RCC.

Introduction

Renal cell carcinoma (RCC) is the most prevalent type of cancer of the urinary system, and is characterized by being a highly malignant tumor (1). Based on its morphological classification, RCC can be mainly divided into three subtypes: i) Kidney renal clear cell carcinoma (KIRC), ii) kidney renal papillary cell carcinoma and iii) suspicious cell malignant tumors. KIRC accounts for >70% of RCC cases (2). RCC is one of the 10 most common cancer types worldwide, causing nearly 140,000 mortalities annually (3). At present, the main treatment for localized RCC is surgical treatment, while immunotherapy, targeted drugs and chemotherapy are the treatment of choice for advanced and metastatic cases (4). Despite advancements in treatment strategies, the 5-year overall survival (OS) rate is just 12% for patients with metastatic KIRC. However, ~16% of patients already have distant metastases upon their initial diagnosis of RCC (5). Therefore, although significant advances in diagnostic techniques and targeted therapies have been made, the prognosis remains poor for the majority of patients (2,6). The high recurrence and incidence rates of KIRC emphasize the urgency to find novel molecular targets for disease treatment.

Ribosomal proteins (RPs) are one of the main components of ribosomes, which play key roles in the regulation of intracellular protein biosynthesis. Specifically, RPs can coordinate interactions between ribosomes, genes, elongation factors and initiators (7). The unique extra-ribosomal effects and functions of distinct RPs have been previously reported (8). These effects are involved in regulating cell proliferation, differentiation and apoptosis, which are crucial

Correspondence to: Dr Bing Zheng, Department of Urology, The Second Affiliated Hospital of Nantong University, 6 North Road, Haierxiang, Nantong, Jiangsu 226001, P.R. China
E-mail: ntzb2008@163.com

Dr Yihui Fan, Department of Pathogenic Biology, School of Medicine, Nantong University, 20 Xisi Road, Chongchuan District, Nantong, Jiangsu 226001, P.R. China
E-mail: fanyihui@ntu.edu.com

*Contributed equally

functions for cell proliferation and development. Although several studies have found abnormal expression patterns of different RPs in a variety of diseases, the specific roles of these proteins and their participation in the underlying molecular mechanisms in the development of human cancer remain unclear.

Ribosomal protein S20 (RPS20) belongs to the S10P family of RPs (9). RPS20 is mainly involved in the regulation of ribosomal RNA processing (10). It is primarily localized in the cytoplasm (11), unlike other RPs, which are usually found in the nucleoli (12-17). Recent evidence suggested that RPS20 is involved in non-ribosomal regulation. RPS20 was shown to be involved in regulating the p53-mouse double minute 2 homolog signaling pathway (18-29). Furthermore, the interaction between GNL1 and RPS20 was found to be capable of regulating cell proliferation (30). RPS20 has also been identified to act as an oncogene in a variety of tumors. However, the specific role of RPS20 in the onset and advancement of RCC remains to be elucidated.

The aim of the present study was to validate the high expression levels of RPS20 in RCC [as observed in The Cancer Genome Atlas (TCGA) database] and to explore its regulatory mechanism. In line with our *in silico* analyses, RPS20 was observed to be highly expressed in RCC tissues. The lentiviral transduction knockdown results further indicated that the inhibition of RPS20 expression could significantly reduce the proliferation, migration, and invasion of RCC cells *in vitro*. Similarly, RPS20 knockdown considerably inhibited the growth of subcutaneous tumors in nude mice. Furthermore, inhibiting RPS20 expression in an RCC cell line reduced the expression of CDK4, cyclin D1 and N-cadherin, and increased the expression of E-cadherin. Lastly, RPS20 was revealed to positively regulate several downstream signaling pathways, including the mTOR and ERK pathways.

Materials and methods

In silico analyses using the Oncomine and TCGA databases. The mRNA expression levels of RPS20 in different tumors were explored using the Oncomine database (31). The threshold and query details were set as follows: Fold-change=2, P=0.05, checked (all) gene ranking and mRNA data. The gene expression profile and clinical records from patients with KIRC were obtained from TCGA website (https://portal.gdc.cancer.gov/), which contained 539 tumor samples and 72 normal samples (32). R software version 3.6.3 with Strawberry Perl was used for data processing. Samples with incomplete information were removed from the datasets before performing statistical analyses.

In silico analysis based on the Gene Expression Profiling Interactive Analysis (GEPIA) database. GEPIA is an open-source database from which expression data of RNA sequencing can be obtained from 10,000 tumor and normal samples (33). Using this tool, the association of high RPS20 expression with the OS and progression-free survival (PFS) of patients with KIRC were analyzed. Moreover, differential gene expression of RPS20 among different tumor types was investigated using the Tumor IMmune Estimation Resource (TIMER) database (https://cistrome.shinyapps.io/timer/).

Clinical patients and tissue samples. In total, 43 RCC tissue samples were collected from patients with renal cancer undergoing partial or radical nephrectomy at The Second Affiliated Hospital of Nantong University (Nantong, China) between January 2017.01 and December 2019, and were compared with their normal tissue counterparts. The tissue samples were immediately stored at -80˚C upon collection. Human studies were approved (approval no. 2021YL012) by the Ethics Committee of The Second Affiliated Hospital of Nantong University (Nantong, China) according to the Declaration of Helsinki of 1964. Written informed consent was provided by all participating patients.

Cell culture. Human RCC cell lines (786-O, ACHN and OS-RC-2) were obtained from the Shanghai Institute of Biological Sciences. ACHN cells were cultured in MEM (Gibco; Thermo Fisher Scientific, Inc.) containing 10% fetal bovine serum (FBS; Gibco; Thermo Fisher Scientific, Inc.), whereas 786-O and OS-RC-2 cells were cultured in RPMI-1640 medium with 10% FBS (Gibco; Thermo Fisher Scientific, Inc.). All cell lines were maintained in a sterile incubator (Thermo Fisher Scientific, Inc.) at 37˚C with 5% CO_2.

RPS20 knockdown using lentiviral transduction. Cells were infected using lentiviral particles containing short hairpin (sh)RPS20 constructs to establish stable RPS20 knockdown cell lines. The shRPS20 sequence used for knockdown was 5'-GATCGTTTCCAGATGAGAATT-3', while the shRNA control sequence used was 5'-TTCTCCCGAACGTGTCACG-3'. RPS20 knockdown lentiviral particles (designated as LV-shRPS20) and negative control (NC) GV248 vector (designated as LV-shNC) were used to infect 786-O and OS-RC-2 cells (MOI=5) following the manufacturer's instructions (Shanghai GeneChem Co., Ltd.). After 48 h of transfection, cells were collected for additional studies. The success of gene knockdown was evaluated by observing the generation of green fluorescent cells under a fluorescence microscope and by using puromycin selection (3 μg/ml). The knockdown efficiency of RPS20 was then confirmed via reverse transcription-quantitative PCR (RT-qPCR) and western blotting.

Western blotting. Protease inhibitors and ice-cold RIPA buffer were premixed with fresh RCC patient tissues or cells to extract proteins. The supernatant was collected, and the concentration of total protein was quantified by utilizing a BCA protein assay kit (Thermo Fisher Scientific, Inc.). Western blotting was performed as previously described (34). The following primary antibodies were used: Anti-RPS20 (cat. no. 15692-1-AP; 1:2,000), anti-β-actin (cat. no. 81115-1-RR; 1:5,000), anti-AKT (cat. no. 60203-2-lg; 1:1,000), anti-phosphorylated (p)-AKT (cat. no. 28731-1-AP; 1:1,000), anti-ERK (cat. no. 51068-1-S-AP; 1:1,000), anti-p-ERK (cat. no. 28733-1-AP; 1:1,000), anti-cyclin D1 (cat. no. 26939-1-AP; 1:2,000), anti-CDK4 (cat. no. 11026-1-AP; 1:1,000), anti-E-cadherin (cat. no. 20874-1-AP; 1:5,000) and anti-N-cadherin (cat. no. 22018-1-AP; 1:1,000; all purchased from ProteinTech Group, Inc.). HRP-conjugated goat anti-rabbit IgG (cat. no. PR3001; 1:5,000) and HRP-conjugated goat anti-mouse IgG (cat. no. PR3002; 1:5,000; both purchased

from ProteinTech Group, Inc.) were the secondary antibodies used in the present study.

Extraction of RNA and RT-qPCR. TRIzol® (Qiagen, Inc.) was used to extract total RNA from RCC cells and tissues. Synthesis of cDNA was performed using the Thermo-Script Reverse Transcription kit (Thermo Fisher Scientific, Inc.), following the reagent manufacturer's instructions. qPCR was performed in 10-μl reactions loaded into 96-well plates with SYBR Green reagent (Takara Bio, Inc.) using the CFX96™ Real-Time PCR system (Bio-Rad Laboratories, Inc.). The thermocycling conditions were as follows: 95°C for 5 min, followed by 40 cycles of 95°C for 15 sec, 60°C for 25 sec and 72°C for 30 sec. Relative gene expression was calculated using the $2^{-\Delta\Delta Cq}$ method (35). Gene expression was normalized using β-*actin* as a housekeeping gene. The following primer sequences were utilized: RPS20 forward, 5'-ATCACCCTAACAAGCCGCAA-3' and reverse, 5'-AGGCATTCGAACTGGTCCTT-3'; and actin forward, 5'-GGGCATGGGTCAGAAGGATT-3' and reverse, 5'-CATGTCGTCCCAGTTGGTGA-3'.

Immunohistochemistry (IHC). Collected RCC and adjacent normal tissues were subjected to IHC analysis. After incubation at 60°C for 60 min, the paraffin-embedded tissue sections were deparaffinized in xylene and then immersed in graded ethanol solutions for hydration. The slides were blocked for 5 min using Ultra V Block (Shilian Boyan Technology Co., Ltd), and the tissue sections were subsequently subjected to overnight incubation at 4°C with an anti-RPS20 primary antibody (1:100; ProteinTech Group, Inc.). Next, the slides were washed with PBS and incubated with a anti-rabbit IgG (cat. no. 15692-1-AP; 1:200; ProteinTech Group, Inc.) secondary antibody at 37°C for 10-30 min. Finally, the tissue samples were stained with diaminobenzidine before evaluation by light microscopy. Specimens were categorized as negative, positive, ++ positive, or +++ positive based on the total of the staining intensity and staining extent scores, which ranged from weak to strong.

Cell Counting Kit (CCK)-8 assay. CCK-8 assay (Dojindo Laboratories, Inc.) was utilized to evaluate the proliferation rate of RCC cells. Cells transduced with either shRPS20 or shNC were seeded in five 96-well plates with a cell density of $3x10^3$ cells/well in triplicates. The proliferation of cells was observed daily for 3 days by incubating the cells with CCK-8 solution (10 μl) and serum-free medium (190 μl) for at 37°C for 2 h. The colorimetric absorbance at 450 nm was estimated using a microplate reader.

Colony formation assay. Transduced OS-RC-2 and 786-O cells, as well as control cells were seeded into six-well plates at a cell density of 800 cells/well. RPMI-1640 with 20% FBS was used for culturing the cells for 7 days at 37°C with 5% CO_2. Colony fixation was performed using 4% paraformaldehyde solution at room temperature for 30 min, followed by washes with PBS and stained using a 0.1% crystal violet solution at room temperature for 5 min, then visualized and counted manually. Colonies consisted of >50 cells.

Wound healing test. Transduced OS-RC-2 and 786-O cells, along with their corresponding control cells, were seeded into six-well plates. When the cell layer reached 100% cell confluency, a scratch wound was made on it with a pipette tip. Cells were cultured in serum-free medium. The migration rates of the two cell groups were evaluated through light microscopy. Images of the cell layers were captured every 6 h.

Invasion assay. Matrigel diluted with serum-free medium (1:6 dilution) was added to the cell culture chamber, and after Matrigel solidification, the cells were cultured. The upper chambers of a Transwell plate (8.0-μm pore size polycarbonate filter) were filled with 200 μl basal serum-free medium, while in the lower chamber, 600 μl complete medium containing 20% FBS was added. Cells were cultured for 1 day at 37°C with 5% CO_2. A cotton swab was used for removing the residual cells from the upper chamber surface. Cells that had migrated to the lower chamber were fixed in paraformaldehyde solution (4%) at room temperature for 30 min, stained using crystal violet (0.1%) at room temperature for 5 min. Then, the mean number of cells was computed by randomly picking five fields under a light microscope and calculating the number of cells in each.

Flow cytometry. Transduced OS-RC-2 and 786-O cells, and their corresponding control cells were seeded into separate dishes for 24 h. Following two washes with ice-cold PBS, the cells were fixed in ethanol solution (70%) overnight at 4°C, trypsinized in PBS (100 μl) and stained at room temperature with propidium iodide (20 μg/ml) for 30 min. Analysis of the cell cycle was performed (ModFit LT 4.1 software) on the different groups of cells using the Beckman MoFlo XDP instrument (A00-1-1102; Beckman Coulter, Inc.).

In vivo xenograft experiments. Female four-week-old BALB/c nude mice (n=10; weight, 16-18 g) were bred at the Animal Research Center of Nantong University. Transduced 786-O-shNC and 786-O-shRPS20 cell resuspension of 100 μl (~5.0x10^6) was collected and implanted in the right armpits of each nude mouse. The animals were housed in microisolator cages with autoclaved bedding with food and water provided *ad libitum*. The mice were maintained on a daily 12/12-h light/dark cycle. The tumor volume and total body weight of the mice were recorded every other week. The tumor volume was calculated based on the following formula: Volume (mm³)=length x width² x 0.52. After the tumors reached a volume of ~1,000 mm³, the mice were euthanized using cervical dislocation, and the tumors were removed, measured and weighed in preparation for further experiments. The animal experiments were approved (approval no. S20210227-041) by the Animal Ethics Committee of Nantong University (Nantong, China) and the experiments were conducted according to the National Institutes of Health Guide for the Care and Use of Laboratory Animals.

Statistical analysis. GraphPad software (version 5.02; GraphPad Software, Inc.) was applied for statistical analyses. The experiments were performed three times for validating their reproducibility. The relationship between RPS20 expression and stage and tumor size was examined using the Kruskal test. The correlation between RPS20 expression and lymph node status and distant metastasis was evaluated by the Wilcox test. Moreover, logistic regression analysis was also applied to
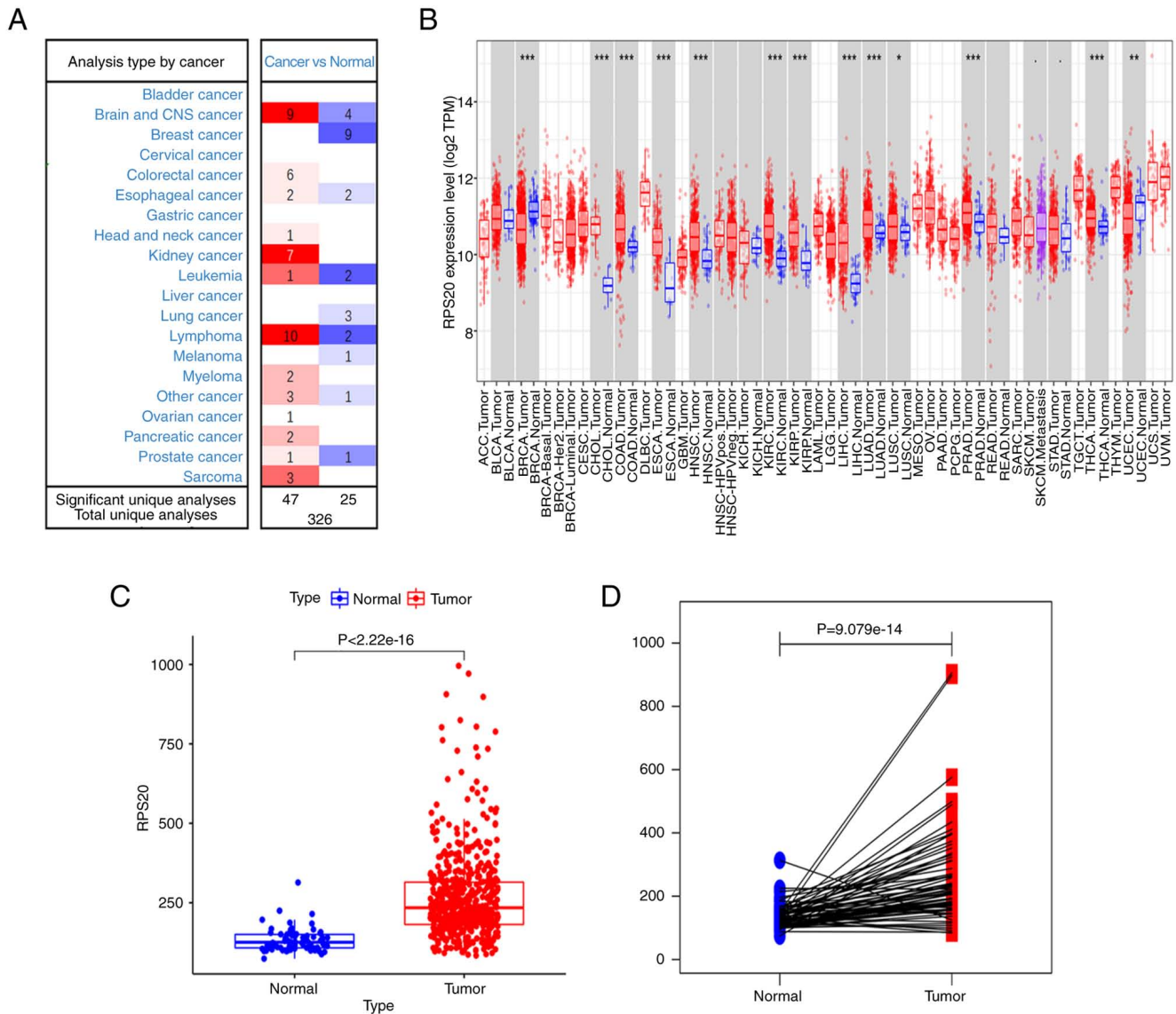
Figure 1. RPS20 is upregulated in patients with kidney renal clear cell carcinoma and acts as a poor prognosis. (A) The Oncomine database was used to evaluate the levels of RPS20 mRNA expression in various cancer types. (B) RPS20 mRNA expression levels in various types of tumors in TCGA dataset, as revealed by the Tumor IMmune Estimation Resource. (C) RPS20 mRNA expression levels for normal renal and KIRC tissues, as visualized by TCGA database. (D) RPS20 mRNA expression levels in normal kidneys and corresponding matched KIRC tissues, as shown by TCGA database. *P<0.05, **P<0.01 and ***P<0.001. RPS20, ribosomal protein S20; TCGA, The Cancer Genome Atlas; ccRCC, clear cell renal cell carcinoma.

estimate the correlation between gene expression and clinicopathological parameters. Univariate and multivariate Cox analyses were adopted to evaluate the value of the RPS20 gene as a prognostic indicator. Kaplan-Meier analysis with the log-rank test was used to conduct the survival study. Statistical comparisons across two groups were performed with a two-tailed unpaired Student's t-test, while one-way ANOVA with Tukey's post hoc test was used for the comparison of multiple groups. *P<0.05 and **P<0.01 were considered to indicate a statistically significant difference.

Results

RPS20 expression in human tumors. Using the Oncomine database to evaluate seven different datasets, higher expression of RPS20 mRNA was found in RCC tissues compared with that in normal samples based on the set threshold. Furthermore, RPS20

was found to be highly expressed in the majority of brain tumors, lymphomas and sarcomas, while its expression was lower in breast tumors and leukemias (Fig. 1A). Similarly, using TIMER, the RPS20 gene was found to be differentially expressed in tumor tissues in comparison with its expression in adjacent normal tissues in patients with RCC (P<0.001; Fig. 1B). Additional analyses using the data retrieved from TCGA database showed that KIRC tissues (n=539) had higher RPS20 mRNA expression levels than adjacent normal tissues (n=72; Fig. 1C and D).

Association of RPS20 expression and clinicopathological variables. The association between RPS20 expression and various clinicopathological characteristics of patients with RCC was investigated, since RPS20 is highly expressed in RCC. Kruskal-Wallis test showed that RPS20 mRNA levels were correlated with disease stage (P<0.001) and tumor size (P<0.001; Fig. 2A and B). Wilcoxon test

Table I. Association between expression of RPS20 and various clinicopathological parameters.

| Clinicopathological variables | Number of cases | Expression level of RPS20 | | χ² | P-value |
		Low	High		
All cases	250	125	125		
Sex				33.865	0.000
Male	99	72	27		
Female	151	53	98		
Age				0.148	0.701
<60	105	51	54		
≥60	145	74	71		
Tumor stage				6.624	0.01
I or II	136	81	55		
III or IV	114	44	71		
T grade				11.306	0.001
T1 or T2	148	84	64		
T3 or T4	102	41	61		
Distant metastasis				0.139	0.709
Negative	209	106	103		
Positive	41	19	21		
Lymph nodes				0.638	0.424
Negative	235	119	116		
Positive	15	6	9		
Years of survival				1.939	0.164
<5	197	94	103		
≥5	53	31	22		

RPS20, ribosomal protein S20.
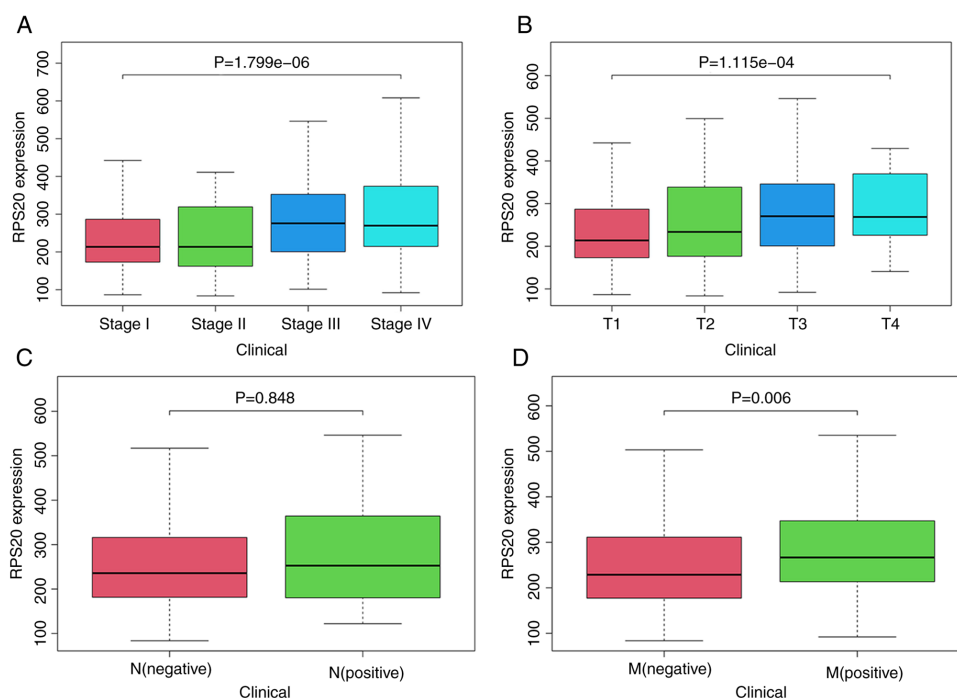
Figure 2. Analysis of the correlation between the expression of RPS20 and various clinicopathological parameters. (A) RPS20 expression in various developmental stages of cancer. (B) RPS20 expression in tumors of varying sizes. (C and D) Quantification of RPS20 expression in tumors in the presence and absence of (C) lymph node metastasis and (D) distant metastasis. RPS20, ribosomal protein S20.
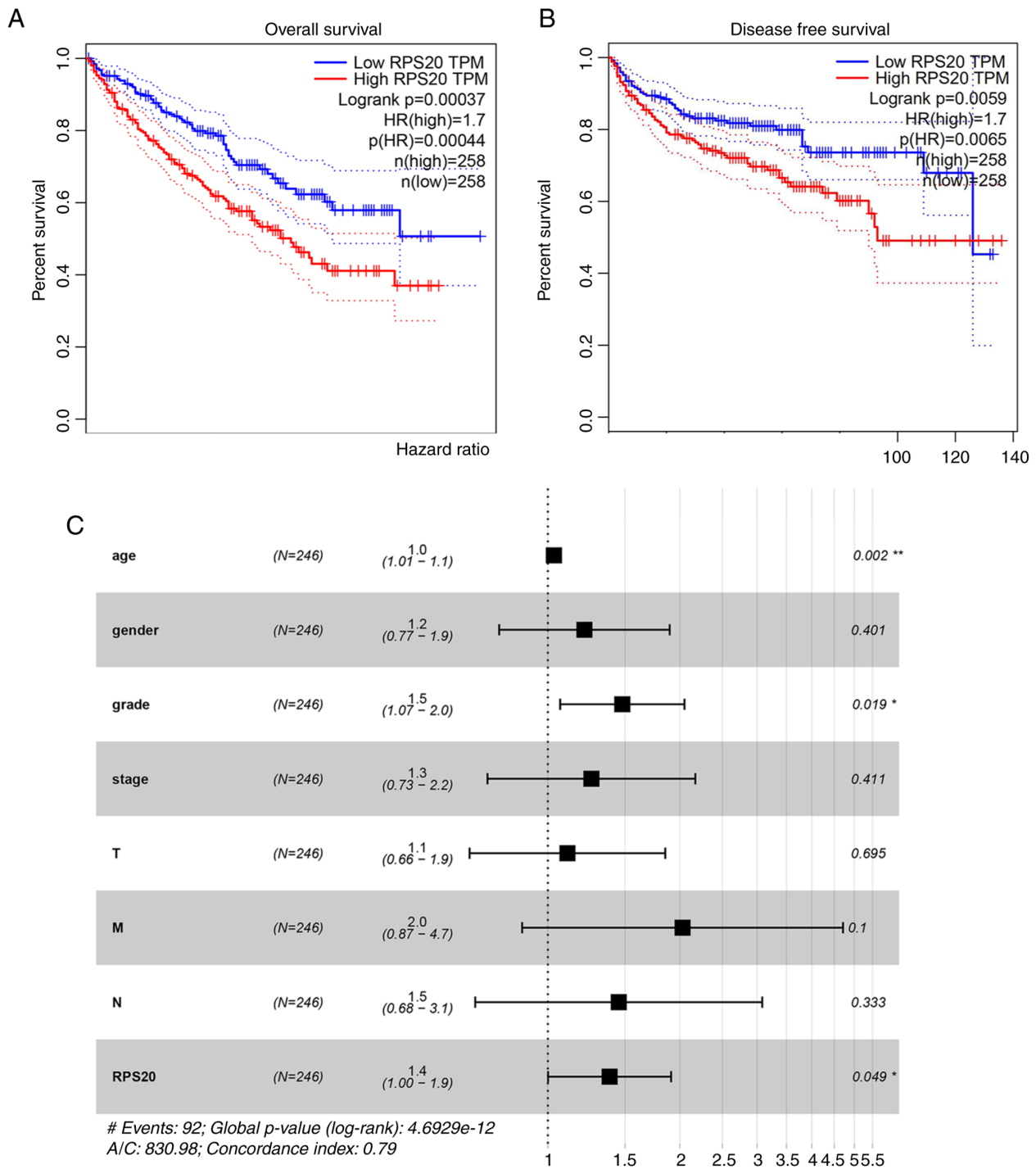
Figure 3. Analysis of the association between RPS20 expression and disease prognosis. (A and B) RPS20 expression was significantly negatively associated with (A) overall survival and (B) disease-free survival, as revealed by analysis of the GEPIA database. (C) Forest map showing the association between RPS20 expression and other clinicopathological parameters. RPS20, ribosomal protein S20; GEPIA, Gene Expression Profiling Interactive Analysis.

showed that high expression of RPS20 was associated with distant metastasis (P=0.006; Fig. 2D). Notably, RPS20 expression had no association with lymph node metastasis (P=0.848). It was hypothesized that this was due to the removal of 289 samples with unknown transfer details (Fig. 2C). Furthermore, logistic regression revealed associations of RPS20 expression with sex (P<0.001), disease stage (P=0.010) and T stage (P=0.001), but not with age, distant metastasis or lymph node metastasis (Table I). Kaplan-Meier survival analysis revealed that RPS20

expression was associated with the OS of patients with RCC (P=0.006; Fig. 4B).

Prognostic potential of RPS20 expression in RCC. Using GEPIA, a negative correlation between RPS20 expression and OS was found [hazard ratio (HR)=1.7; P=0.00044; Fig. 3A] and DFS (HR=1.7; P=0.0065; Fig. 3B). To validate these findings, data from TCGA was further analyzed. Univariate Cox analysis revealed that OS was associated with RPS20 expression (HR=1.03; P<0.05), age (HR=1.02; P<0.05), disease stage

Table II. Univariate and multivariate Cox analyses of clinicopathological parameters and overall survival in patients with clear cell renal cell carcinoma.

Clinicopathological parameters	Univariate analysis		Multivariate analysis	
	HR (95% CI)	P-value	HR (95% CI)	P-value
Age	1.02 (1.00-1.04)	0.012	1.03 (1.01-1.05)	0.001
Sex	1.01 (0.67-1.54)	0.951	1.21 (0.77-1.90)	0.400
Grade	2.24 (1.68-2.99)	0.000	1.48 (1.07-2.05)	0.018
Stage	1.86 (1.54-2.25)	0.000	1.26 (0.73-2.17)	0.411
T	1.94 (1.54-2.46)	0.000	1.11 (0.66-1.85)	0.695
N	4.07 (2.63-6.30)	0.000	2.03 (0.87-4.71)	0.099
M	2.93 (1.52-5.67)	0.001	1.45 (0.68-3.08)	0.333
Ribosomal protein S20	1.00 (1.00-1.00)	0.025	1.38 (1.00-1.90)	0.049

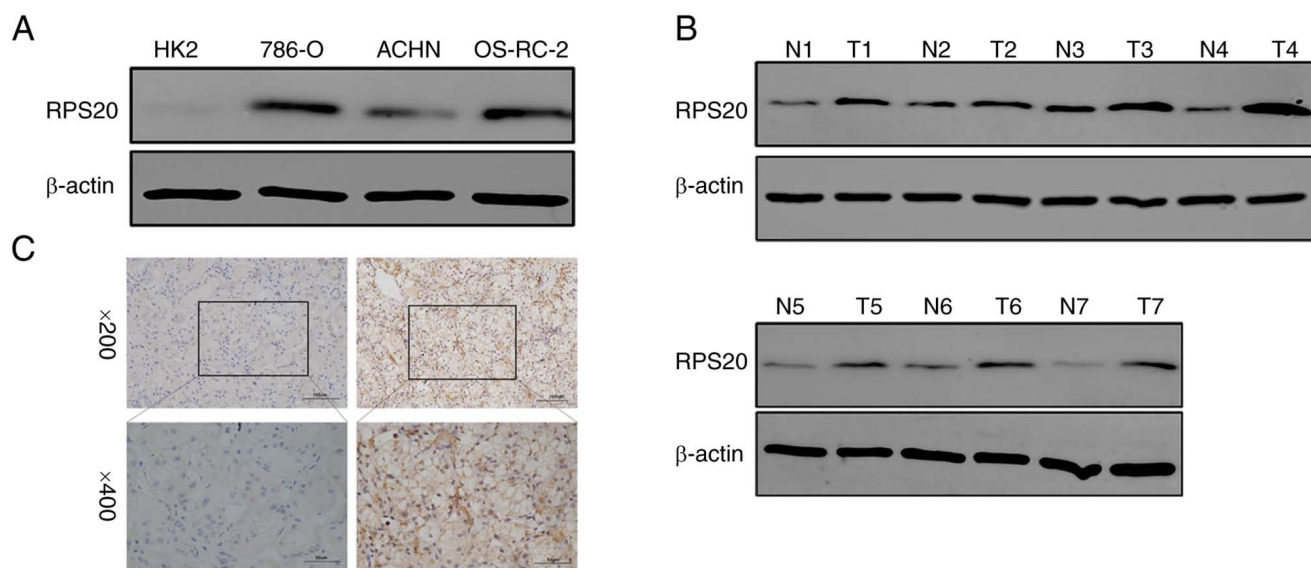HR, hazard ration; CI, confidence interval.

Figure 4. RPS20 expression is markedly upregulated in RCC tissues and cell lines. (A) RPS20 protein expression level in RCC cell lines and normal epithelial cells of the renal tubule. (B) RPS20 was upregulated in samples from patients with clear cell RCC compared with its expression in adjacent normal tissues. (C) Immunohistochemical analysis of RPS20 in RCC and adjacent normal tissues. The results are presented as the mean ± standard deviation. RPS20, ribosomal protein S20; RCC, renal cell carcinoma.

(HR=1.86; P<0.001), tumor size (HR=1.94; P<0.001), lymph node status (HR=4.07; P<0.001) and distant metastasis (HR=2.93; P<0.01) (Table II). Multivariate analysis revealed that age (HR=1.03; P<0.05) and RPS20 expression (HR=1.38; P<0.05) were independent prognostic values (Table II and Fig. 3C).

Expression of RPS20 in KIRC tissues. The differential expression of RPS20 was validated via western blotting and IHC in various RCC cell lines as well as 43 paired RCC and normal tissue samples. High expression of RPS20 in the three analyzed RCC cell lines and renal cell tissues were revealed by western blotting (Fig. 4A and B). Similarly, the IHC results showed a significant upregulation of RPS20 in RCC samples (Fig. 4C).

RPS20 is downregulated in 786-O and OS-RC-2 RCC cell lines. To investigate the role of RPS20 in RCC, shRNA constructs for RPS20 were generated. The 786-O and OS-RC-2 KIRC cell lines were transduced with RPS20 shRNA and control lentiviral particles to construct stable RPS20 knockdown cell lines. Successful knockdown of RPS20 was confirmed by RT-qPCR which showed a 90% decrease in the expression levels of RPS20 mRNA in the aforementioned cell lines compared with those in the control vector group (P<0.01; Fig. 5A and B). Similarly, RPS20 protein levels were measured by western blotting, and the knockdown efficiency was found to exceed 50% (Fig. 5C and D).

Knockdown of RPS20 suppresses the proliferation and mobility of RCC cells in vitro. To further elucidate the effect of RPS20 on the proliferation of RCC cells, CCK-8 assays were performed on the knockdown cell lines generated in the present study. The results showed that the proliferation
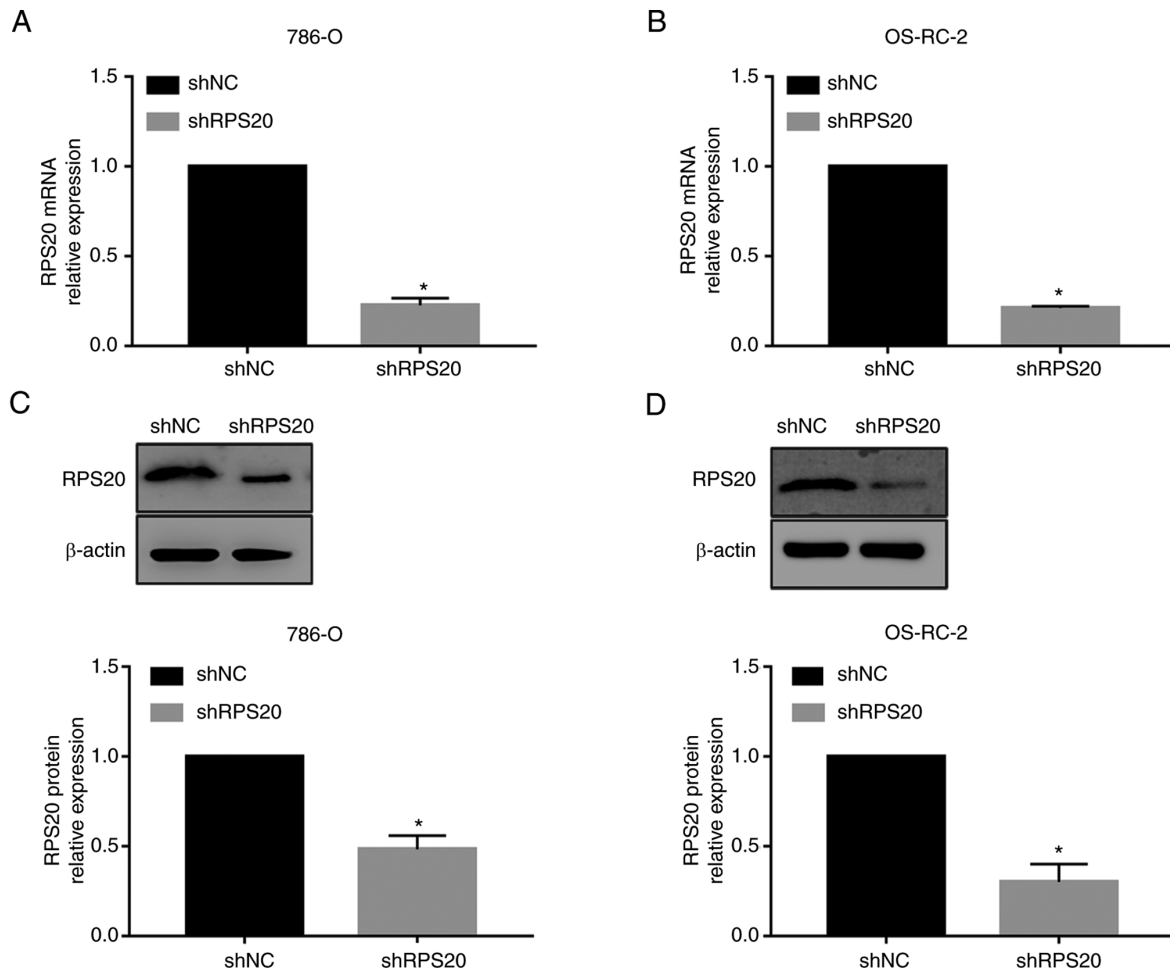
Figure 5. Validation of RPS20 knockdown in 786-O and OS-RC-2 cells. (A and B) RPS20 knockdown efficiency in (A) 786-O and (B) OS-RC-2 cells was determined by reverse transcription-quantitative PCR. (C and D) RPS20 protein expression level was considerably decreased in the short hairpin RPS20 group in (A) 786-O and (B) OS-RC-2 cells, as determined by western blotting. The results are presented as the mean ± standard deviation. *P<0.05. RPS20, ribosomal protein S20. short hairpin; NC, negative control.

of RPS20 knockdown cell lines was significantly inhibited compared with that of control cells (Fig. 6A). Colony formation assay was used to assess the possible function of RPS20 in cell proliferation. Similarly, RPS20 knockdown cells formed fewer colonies than control cells (Fig. 6B and E). Furthermore, wound-healing assays were performed on the RPS20 knockdown cell lines (Fig. 6C and F). Knocking down RPS20 considerably led to inhibition of RCC cell invasion and migration, according to the results of Transwell assays (Fig. 6D and G). Consistent with these findings, RPS20 knockdown cells displayed a significantly increased E-cadherin level and a decreased N-cadherin level (Fig. 6H and I).

RPS20 knockdown induces cell cycle arrest. To investigate the mechanism by which RPS20 contributed to the proliferation of 786-O and OS-RC-2 cells, cell cycle analysis was performed. The results showed that the proportion of cells in the G_0/G_1 phase was 74.86 and 65.23% in LV-shRPS20 786-O and OS-RC-2 cells, respectively, while it was 42.35 and 45.41% in LV-shNC 786-O and OS-RC-2 cells, respectively (P<0.05; Fig. 7A and B). These data suggested that the cell cycle was arrested in G_0/G_1 phase after RPS20 was knocked down. Consistent with these results, the expression levels of the cell

cycle-associated proteins CDK4 and cyclin D1 were found to be lower in shRPS20 786-O and OS-RC-2 cells (Fig. 7C-E).

RPS20 knockdown inhibits the mTOR and ERK signaling pathways. To explore the signaling pathways that may be regulated by RPS20, the effects of knocking down RPS20 in the mTOR and ERK signaling pathways were evaluated using western blotting. The results revealed that knocking down RPS20 considerably inhibited the phosphorylation of AKT and ERK, while total AKT and ERK protein levels were not affected (Fig. 8A and B). These results suggested a key role of RPS20 in the ERK-MAPK and AKT-mTOR signaling pathways.

RPS20 promotes tumor development in vivo. To further support the present *in vitro* experiments, the current study further analyzed *in vivo* whether RPS20 shRNA may affect tumorigenesis. For establishing xenograft mice models, cell suspensions of the aforementioned RPS20 knockdown cell lines were implanted into both armpits of each nude mouse. The results revealed that tumor growth was considerably inhibited in the RPS20 knockdown group compared with that of the control group (Fig. 9A and B). Consistently, tumor weight in the RPS20 knockdown group
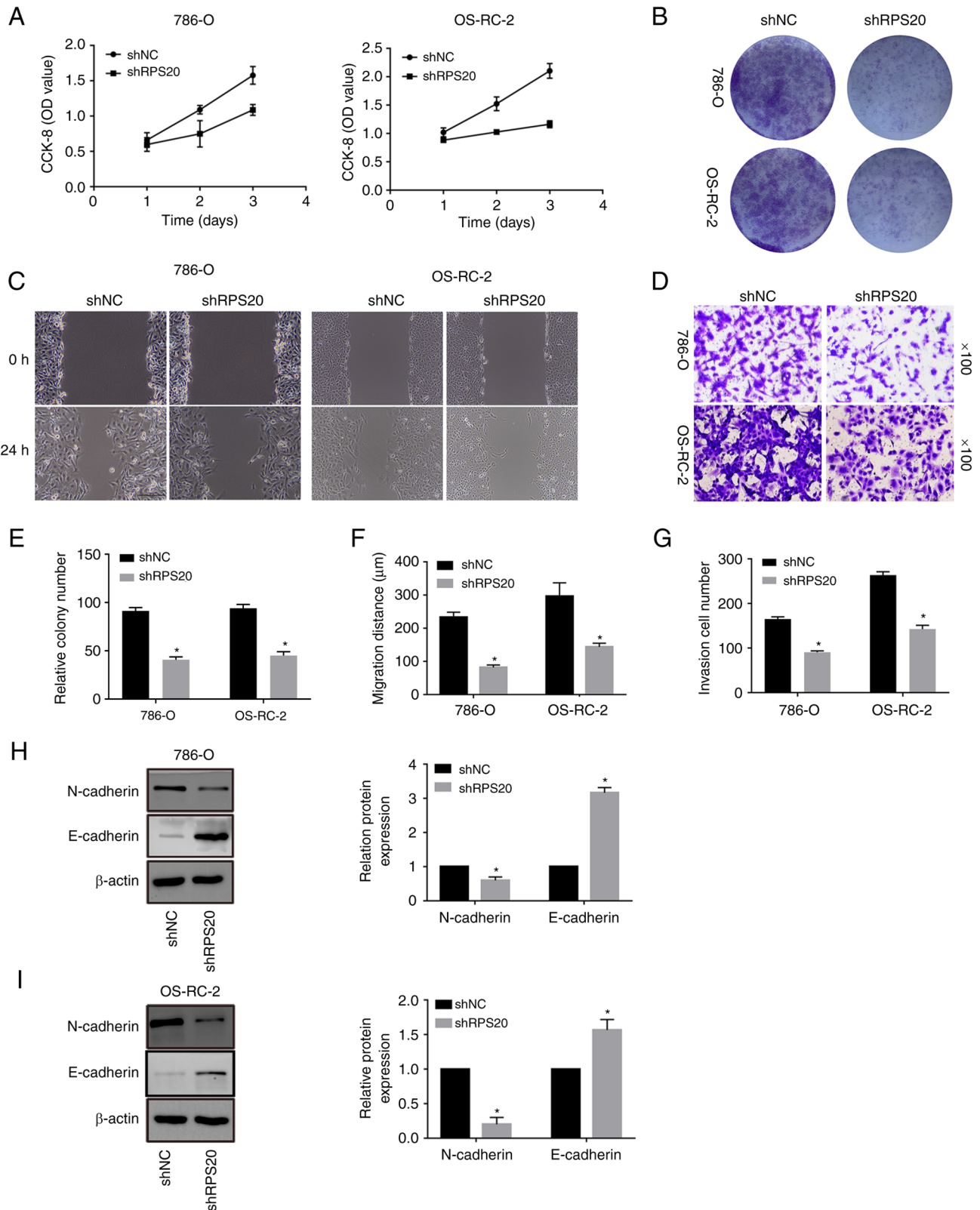
Figure 6. RPS20 promotes the proliferation, colony formation and invasion of RCC cells *in vitro*. (A) Cell Counting Kit-8 assay was utilized to evaluate the proliferation of 786-O and OSRC-2 cells. (B and E) Knocking down RPS20 inhibited the colony formation ability of 786-O and OS-RC-2 cells. (C and F) For assessing the effects of RPS20 knockdown on RCC cell migration, wound healing assays were utilized. (D and G) Evaluation of the effects of RPS20 knockdown on the migration of RCC cells via Transwell assays. (H and I) Western blot analysis was used to semi-quantitatively detect the protein levels of the epithelial-mesenchymal transition markers E-cadherin and N-cadherin. The results are presented as the mean ± standard deviation. *P<0.05. RPS20, ribosomal protein S20; RCC, renal cell carcinoma. short hairpin; NC, negative control.

was significantly lower compared with that of the control group (Fig. 9C and D). Overall, these results indicated that

RPS20 knockdown may lead to the inhibition of RCC tumor cell proliferation *in vivo*.
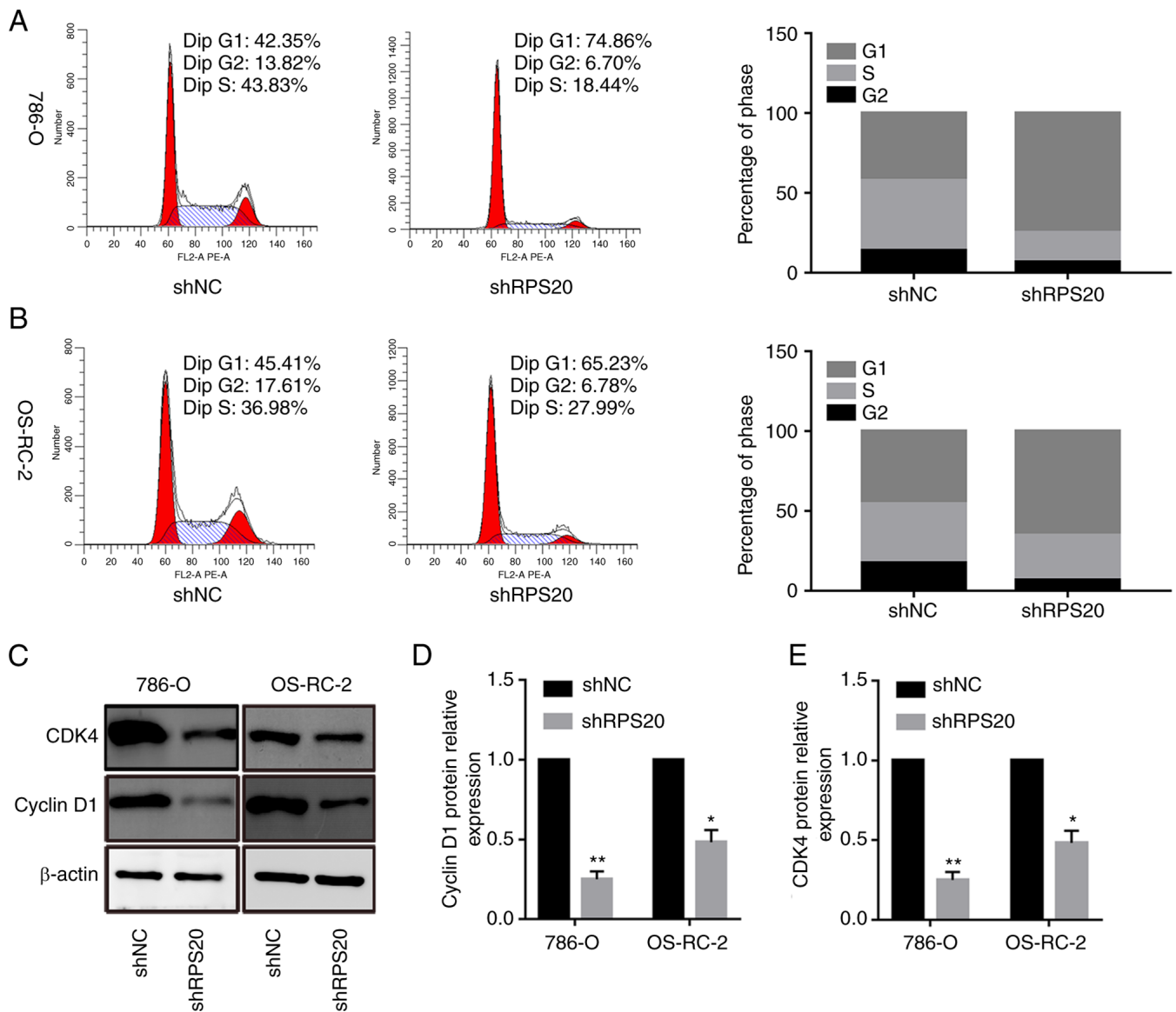
Figure 7. RPS20 knockdown inhibits the proliferation of renal cell carcinoma cells. (A and B) Cell cycle distribution in (A) 786-O and (B) OS-RC-2 cells was analyzed by flow cytometry. (C-E) CDK4 and cyclin D1 protein levels were measured by western blotting. The results are presented as the mean ± standard deviation. *P<0.05 and **P<0.01. RPS20, ribosomal protein S20; sh-, short hairpin; NC, negative control.

Discussion

Kidney cancer is a heterogeneous disease. Current evidence suggests that the majority of RCCs develop due to several factors, including dysregulation of hypoxia-inducible factor signaling, mutations in key histone and chromatin-modifying enzymes, and metabolic reprogramming of cellular metabolism (36,37). While advancements in diagnostic techniques and targeted therapies have been achieved in recent decades, disease prognosis remains unsatisfactory. Thus, screening for new biomarkers may offer novel strategies for diagnosing and treating KIRC. The rapid advancement of high-throughput sequencing technologies and bioinformatics techniques may provide novel methods for diagnosing and treating KIRC.

　　Various RPs have critical importance in the onset and progression of different human tumors. For example, RPL11 interacts with Myc and suppresses its transcriptional

activity (38), while RP S29 induces cell apoptosis by regulating p53 and Bcl-2 (39). Moreover, abnormal RP expression can lead to non-neoplastic diseases such as hemochromatosis and anemia (40). Previous research has slowly unveiled the role of RPS20 outside of the ribosome. Cell proliferation can be regulated by human nucleolar GNL1 and RPS20 interaction (30). The Mdm2-p53-MdmX network may be controlled by the ribosomal proteins RPL37, RPS15 and RPS20 (41). RPS20 mutations enhance the risk of developing hereditary non-polyposis colorectal cancer (42). According to the findings of a recent bioinformatics study, the member of the ribosomal family known as RPS20 may be helpful as a prognostic predictor in patients diagnosed with ccRCC (43). The function of RPS20 in ccRCC still needs to be fully understood. The findings of the present study suggested that RPS20 is upregulated in ccRCC tissues and cell lines, associated with clinicopathological characteristics (grade, stage) in ccRCC patients. Furthermore, it was found that the knockdown of
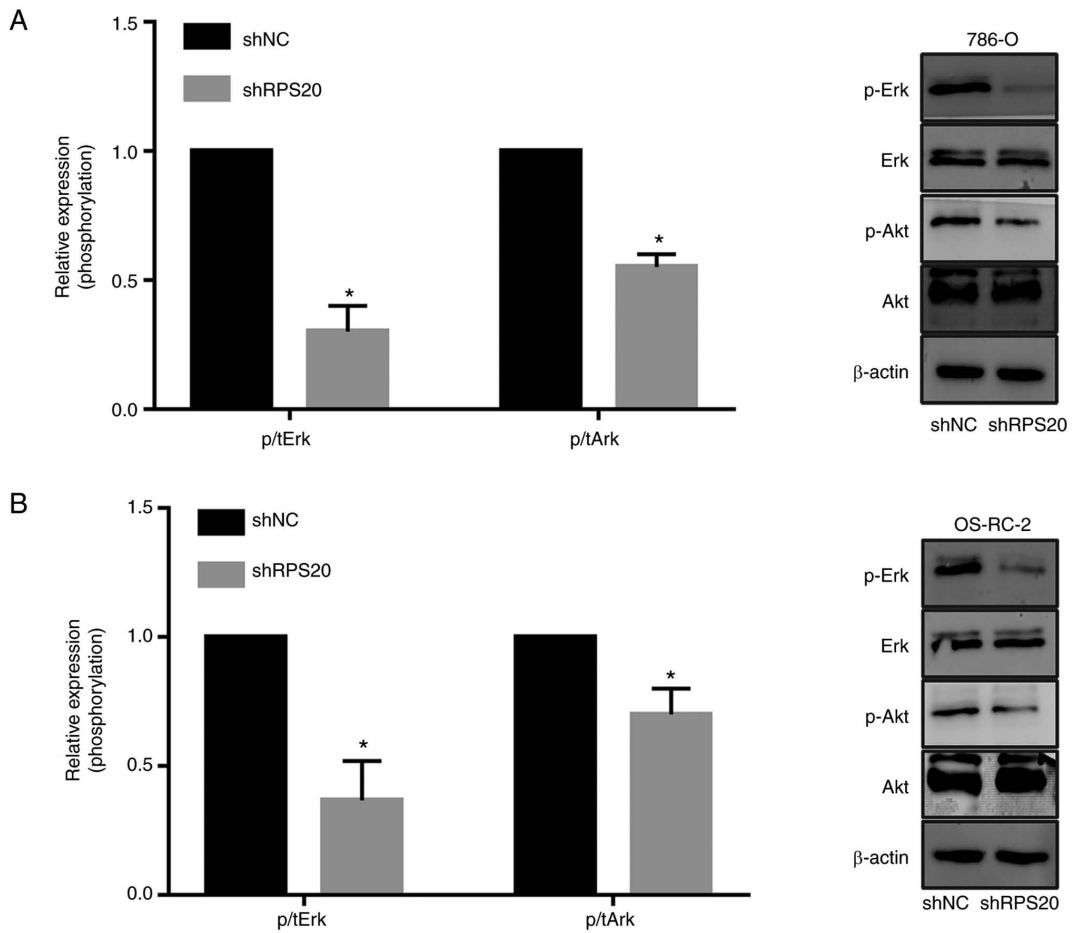
Figure 8. RPS20 knockdown inhibits the MAPK-ERK and PI3K-AKT signaling pathways. The protein expression levels of p-AKT and p-ERK in 786-O and OS-RC-2 cells were analyzed via western blotting. Knocking down RPS20 inhibited the AKT-mTOR and ERK-MAPK signaling pathways in (A) 786-O and (B) OS-RC-2 cells. The results are presented as the mean ± standard deviation. *$P<0.05$. RPS20, ribosomal protein S20; p, phosphorylated; sh-, short hairpin; NC, negative control.
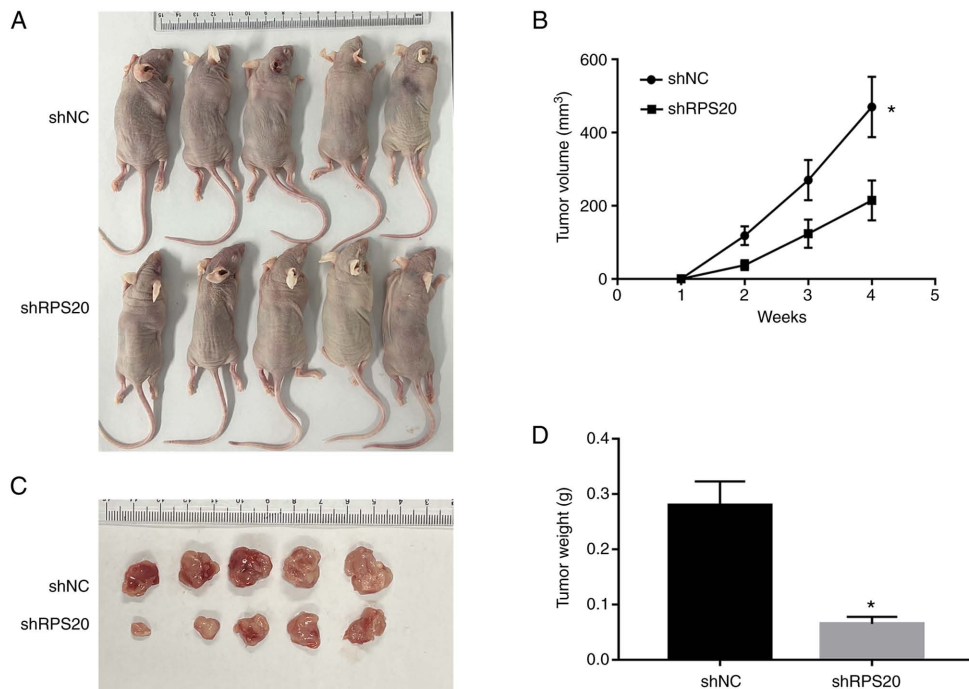

Figure 9. RPS20 knockdown inhibits tumor growth in nude mice. (A) RPS20 knockdown led to a decrease in tumor volume. (B) Representative tumor images of short hairpin RPS20 and control-treated nude mice. (C and D) Measurement of changes in volume and weight of tumors at different time points following transplantation. The results are presented as the mean ± standard deviation. *$P<0.05$. RPS20, ribosomal protein S20.

RPS20 may limit cell proliferation, migration, and invasion via inhibition of MAPK and AKT signaling pathways.

The multistep and intricate process of tumor invasion and metastasis has become a significant barrier to the clinical treatment of several malignancies (44,45). Furthermore, metastasis can result in ccRCC treatment failure, which lowers 5-year survival rates (5). As a result, limiting cell migration and invasion can effectively control cancer cell spread. According to the results of the current investigation, migration and invasion assays revealed that RPS20 knockdown significantly reduced the invasion and metastasis of ccRCC cells.

Additionally, patients with ccRCC have a poor prognosis when MAPK and AKT signaling pathways are activated (46). The MAPK pathway comprises three proteins: ERK, JNK and p38. ERK is a crucial signal transducer for cell survival, and JNK and p38 help cells learn to invade and migrate (47). There is growing evidence that MAPKs may stop tumor invasion and metastasis in various tumor types (48,49). AKT signaling is additionally engaged in numerous biological processes, including glucose metabolism and cell cycle, particularly in cancer cells (50). AKT signaling is suppressed in ccRCC cells, which reduces invasion and metastasis (51). In the present study, it was demonstrated that RPS20 knockdown suppresses MAPK and AKT signaling in ccRCC.

To conclude, the current results clearly demonstrated that RPS20 was upregulated in human RCC tissues. Mechanistically, it was found that RPS20 protein could promote not only the proliferation and migration but also the invasion of RCC cells via regulating the AKT-mTOR and ERK-MAPK signaling pathways. However, the present study was based on the hypothesis that RPS20 has dual functions as a ribosomal component and signal transducer. Consequently, no experiments were conducted to investigate whether RPS20 mediated direct activation of the ERK-MAPK and AKT-mTOR signaling pathways. In future studies, the specific mechanisms by which RPS20 affects the aforementioned pathways will be investigated.

Availability of data and materials

The datasets used and/or analyzed during the current study are available from the corresponding author on reasonable request.

Authors' contributions

CS, ZC, YZ, WX and RP performed the experiments. CS and BZ confirm the authenticity of all the raw data. JJ, YF and WZ analyzed the data. CS and ZC wrote the manuscript. BZ designed this study and polished the manuscript. All authors read and approved the final manuscript.

Ethics approval and consent to participate

Human studies were approved (approval no. 2021YL012) by the Ethics Committee of The Second Affiliated Hospital of Nantong University (Nantong, China) according to the Declaration of Helsinki of 1964. Written informed consent was provided by all participating patients. The animal experiments were approved (approval no. S20210227-041) by the Animal Ethics Committee of Nantong University (Nantong, China) and the experiments were conducted according to the National Institutes of Health Guide for the Care and Use of Laboratory Animals.

Patient consent for publication

Not applicable.

Competing interests

The authors declare that they have no competing interests.

References

1. Miller KD, Nogueira L, Mariotto AB, Rowland JH, Yabroff KR, Alfano CM, Jemal A, Kramer JL and Siegel RL: Cancer treatment and survivorship statistics, 2019. CA Cancer J Clin 69: 363-385, 2019.
2. Fernández-Pello S, Hofmann F, Tahbaz R, Marconi L, Lam TB, Albiges L, Bensalah K, Canfield SE, Dabestani S, Giles RH, *et al*: A systematic review and meta-analysis comparing the effectiveness and adverse effects of different systemic treatments for non-clear cell renal cell carcinoma. Eur Urol 71: 426-436, 2017.
3. Rhoades Smith KE and Bilen MA: A review of papillary renal cell carcinoma and MET inhibitors. Kidney Cancer 3: 151-161, 2019.
4. Chen VJ, Hernandez-Meza G, Agrawal P, Zhang CA, Xie L, Gong CL, Hoerner CR and Srinivas S, Oermann EK and Fan AC: Time on therapy for at least three months correlates with overall survival in metastatic renal cell carcinoma. Cancers (Basel) 11: 1000, 2019.
5. Siegel RL, Miller KD and Jemal A: Cancer statistics, 2018. CA Cancer J Clin 68: 7-30, 2018.
6. Gao C, Guo X, Xue A, Ruan Y, Wang H and Gao X: High intratumoral expression of eIF4A1 promotes epithelial-to-mesenchymal transition and predicts unfavorable prognosis in gastric cancer. Acta Biochim Biophys Sin (Shanghai) 52: 310-319, 2020.
7. Ruggero D and Pandolfi PP: Does the ribosome translate cancer? Nat Rev Cancer 3: 179-192, 2003.
8. Lindström MS: Emerging functions of ribosomal proteins in gene-specific transcription and translation. Biochem Biophys Res Commun 379: 167-170, 2009.
9. Chu W, Presky DH, Swerlick RA and Burns DK: Human ribosomal protein S20 cDNA sequence. Nucleic Acids Res 21: 1672, 1993.
10. O'Donohue MF, Choesmel V, Faubladier M, Fichant G and Gleizes PE: Functional dichotomy of ribosomal proteins during the synthesis of mammalian 40S ribosomal subunits. J Cell Biol 190: 853-866, 2010.
11. Tai LR, Chou CW, Wu JY, Kirby R and Lin A: Late-assembly of human ribosomal protein S20 in the cytoplasm is essential for the functioning of the small subunit ribosome. Exp Cell Res 319: 2947-2953, 2013.
12. Ko JR, Wu JY, Kirby R, Li IF and Lin A: Mapping the essential structures of human ribosomal protein L7 for nuclear entry, ribosome assembly and function. FEBS Lett 580: 3804-3810, 2006.
13. Chen IJ, Wang IA, Tai LR and Lin A: The role of expansion segment of human ribosomal protein L35 in nuclear entry, translation activity, and endoplasmic reticulum docking. Biochem Cell Biol 86: 271-277, 2008.

14. Schmidt C, Lipsius E and Kruppa J: Nuclear and nucleolar targeting of human ribosomal protein S6. Mol Biol Cell 6: 1875-1885, 1995.
15. Shu-Nu C, Lin CH and Lin A: An acidic amino acid cluster regulates the nucleolar localization and ribosome assembly of human ribosomal protein L22. FEBS Lett 484: 22-28, 2000.
16. Da Costa L, Tchernia G, Gascard P, Lo A, Meerpohl J, Niemeyer C, Chasis JA, Fixler J and Mohandas N: Nucleolar localization of RPS19 protein in normal cells and mislocalization due to mutations in the nucleolar localization signals in 2 Diamond-Blackfan anemia patients: Potential insights into pathophysiology. Blood 101: 5039-5045, 2003.
17. Antoine M, Reimers K, Wirz W, Gressner AM, Müller R and Kiefer P: Identification of an unconventional nuclear localization signal in human ribosomal protein S2. Biochem Biophys Res Commun 335: 146-153, 2005.
18. Ferreira-Cerca S, Pöll G, Gleizes PE, Tschochner H and Milkereit P: Roles of eukaryotic ribosomal proteins in maturation and transport of pre-18S rRNA and ribosome function. Mol Cell 20: 263-275, 2005.
19. Rouquette J, Choesmel V and Gleizes PE: Nuclear export and cytoplasmic processing of precursors to the 40S ribosomal subunits in mammalian cells. EMBO J 24: 2862-2872, 2005.
20. Zhang Y and Lu H: Signaling to p53: Ribosomal proteins find their way. Cancer Cell 16: 369-377, 2009.
21. Boulon S, Westman BJ, Hutten S, Boisvert FM and Lamond AI: The nucleolus under stress. Mol Cell 40: 216-227, 2010.
22. Zhang Y, Wolf GW, Bhat K, Jin A, Allio T, Burkhart WA and Xiong Y: Ribosomal protein L11 negatively regulates oncoprotein MDM2 and mediates a p53-dependent ribosomal-stress checkpoint pathway. Mol Cell Biol 23: 8902-8912, 2003.
23. Dai MS and Lu H: Inhibition of MDM2-mediated p53 ubiquitination and degradation by ribosomal protein L5. J Biol Chem 279: 44475-44482, 2004.
24. Jin A, Itahana K, O'Keefe K and Zhang Y: Inhibition of HDM2 and activation of p53 by ribosomal protein L23. Mol Cell Biol 24: 7669-7680, 2004.
25. Zhang Y, Wang J, Yuan Y, Zhang W, Guan W, Wu Z, Jin C, Chen H, Zhang L, Yang X and He F: Negative regulation of HDM2 to attenuate p53 degradation by ribosomal protein L26. Nucleic Acids Res 38: 6544-6554, 2010.
26. Chen D, Zhang Z, Li M, Wang W, Li Y, Rayburn ER, Hill DL, Wang H and Zhang R: Ribosomal protein S7 as a novel modulator of p53-MDM2 interaction: Binding to MDM2, stabilization of p53 protein, and activation of p53 function. Oncogene 26: 5029-5037, 2007.
27. Xiong X, Zhao Y, He H and Sun Y: Ribosomal protein S27-like and S27 interplay with p53-MDM2 axis as a target, a substrate and a regulator. Oncogene 30: 1798-1811, 2011.
28. Sun XX, DeVine T, Challagundla KB and Dai MS: Interplay between ribosomal protein S27a and MDM2 protein in p53 activation in response to ribosomal stress. J Biol Chem 286: 22730-22741, 2011.
29. Frum R, Busby SA, Ramamoorthy M, Deb S, Shabanowitz J, Hunt DF and Deb SP: HDM2-binding partners: Interaction with translation elongation factor EF1alpha. J Proteome Res 6: 1410-1417, 2007.
30. Krishnan R, Boddapati N and Mahalingam S: Interplay between human nucleolar GNL1 and RPS20 is critical to modulate cell proliferation. Sci Rep 8: 11421, 2018.
31. Rhodes DR, Kalyana-Sundaram S, Mahavisno V, Varambally R, Yu J, Briggs BB, Barrette TR, Anstet MJ, Kincead-Beal C, Kulkarni P, et al: Oncomine 3.0: Genes, pathways, and networks in a collection of 18,000 cancer gene expression profiles. Neoplasia 9: 166-180, 2007.
32. Lánczky A, Nagy Á, Bottai G, Munkácsy G, Szabó A, Santarpia L and Győrffy B: miRpower: A web-tool to validate survival-associated miRNAs utilizing expression data from 2178 breast cancer patients. Breast Cancer Res Treat 160: 439-446, 2016.
33. Tang Z, Li C, Kang B, Gao G, Li C and Zhang Z: GEPIA: A web server for cancer and normal gene expression profiling and interactive analyses. Nucleic Acids Res 45: W98-W102, 2017.
34. Zheng B, Mao JH, Qian L, Zhu H, Gu DH, Pan XD, Yi F and Ji DM: Pre-clinical evaluation of AZD-2014, a novel mTORC1/2 dual inhibitor, against renal cell carcinoma. Cancer Lett 357: 468-475, 2015.
35. Livak KJ and Schmittgen TD: Analysis of relative gene expression data using real-time quantitative PCR and the 2(-Delta Delta C(T)) method. Methods 25: 402-408, 2001.
36. Wettersten HI, Aboud OA, Lara PN and Weiss RH: Metabolic reprogramming in clear cell renal cell carcinoma. Nat Rev Nephrol 13: 410-419, 2017.
37. Xie M, Ma T, Xue J, Ma H, Sun M, Zhang Z, Liu M, Liu Y, Ju S, Wang Z and De W: The long intergenic non-protein coding RNA 707 promotes proliferation and metastasis of gastric cancer by interacting with mRNA stabilizing protein HuR. Cancer Lett 443: 67-79, 2019.
38. Dai MS, Sears R and Lu H: Feedback regulation of c-Myc by ribosomal protein L11. Cell Cycle 6: 2735-2741, 2007.
39. Khanna N, Sen S, Sharma H and Singh N: S29 ribosomal protein induces apoptosis in H520 cells and sensitizes them to chemotherapy. Biochem Biophys Res Commun 304: 26-35, 2003.
40. Warner JR and McIntosh KB: How common are extraribosomal functions of ribosomal proteins? Mol Cell 34: 3-11, 2009.
41. Daftuar L, Zhu Y, Jacq X and Prives C: Ribosomal proteins RPL37, RPS15 and RPS20 regulate the Mdm2-p53-MdmX network. PLoS One 8: e68667, 2013.
42. Nieminen TT, O'Donohue MF, Wu Y, Lohi H, Scherer SW, Paterson AD, Ellonen P, Abdel-Rahman WM, Valo S, Mecklin JP, et al: Germline mutation of RPS20, encoding a ribosomal protein, causes predisposition to hereditary nonpolyposis colorectal carcinoma without DNA mismatch repair deficiency. Gastroenterology 147: 595-598.e5, 2014.
43. Li CX, Chen J, Xu ZG, Yiu WK and Lin YT: The expression and prognostic value of RNA binding proteins in clear cell renal cell carcinoma. Transl Cancer Res Dec 9: 7415-7431, 2020.
44. Uekita T and Sakai R: Roles of CUB domain-containing protein 1 signaling in cancer invasion and metastasis. Cancer Sci 102: 1943-1948, 2011.
45. Friedl P, Locker J, Sahai E and Segall JE: Classifying collective cancer cell invasion. Nat Cell Biol 14: 777-783, 2012.
46. Fan D, Liu Q, Wu F, Liu N, Qu H, Yuan Y, Li Y, Gao H, Ge J, Xu Y, et al: Prognostic significance of PI3K/AKT/mTOR signaling pathway members in clear cell renal cell carcinoma. PeerJ 8: e9261, 2020.
47. Igaki T, Pagliarini RA and Xu T: Loss of cell polarity drives tumor growth and invasion through JNK activation in Drosophila. Curr Biol 16: 1139-1146, 2006.
48. Chen PN, Hsieh YS, Chiang CL, Chiou HL, Yang SF and Chu SC: Silibinin inhibits invasion of oral cancer cells by suppressing the MAPK pathway. J Dent Res 85: 220-225, 2006.
49. Reddy KB, Nabha SM and Atanaskova N: Role of MAP kinase in tumor progression and invasion. Cancer Metastasis Rev 22: 395-403, 2003.
50. Matsushima-Nishiwaki R, Toyoda H, Takamatsu R, Yasuda E, Okuda S, Maeda A, Kaneoka Y, Yoshimi N, Kumada T and Kozawa O: Heat shock protein 22 (HSPB8) reduces the migra-tion of hepatocellular carcinoma cells through the suppression of the phosphoinositide 3-kinase (PI3K)/AKT pathway. Biochim Biophys Acta Mol Basis Dis 1863: 1629-1639, 2017.
51. Wang L, Fang Z, Gao P and Zheng J: GLUD1 suppresses renal tumorigenesis and development via inhibiting PI3K/Akt/mTOR pathway. Front Oncol 12: 975517, 2022.